ELSEVIER

Microelectronic Engineering 43–44 (1998) 423–429

MICROELECTRONIC ENGINEERING

Optical absorption and band gap shift of n-doped $Al_xGa_{1-x}As$ alloys grown by MBE

A. Ferreira da Silva[a,*], C. Persson[a], K.-F. Berggren[a], I. Pepe[b], A. Santos Alves[b], A.G. de Oliveira[c]

[a]*Linköping University, Department of Physics and Measurement Technology, S-581 83 Linköping, Sweden*
[b]*Instituto de Física, Universidade Federal da Bahia, 40210-340 Salvador, Bahia, Brazil*
[c]*Departamento de Física-ICEx, Universidade Federal de Minas Gerais, 30161-970 Belo Horizonte, MG, Brazil*

Abstract

We have investigated the band gap shift of Si-doped $Al_xGa_{1-x}As$ alloys as a function of both silicon concentration and Al composition. Correlation and impurity scattering effects were included in the theoretical model. The optical absorption of $Al_{0.3}Ga_{0.7}As$:Si at the fundamental band gap energy has been measured by a photoacoustic spectroscopy technique. We found the energy gap at about 1.8 eV. The samples were grown by molecular beam epitaxy and the Al fraction was measured by reflection high energy electro-diffraction technique. © 1998 Published by Elsevier Science B.V. All rights reserved.

Keywords: Doped AlGaAs alloys; Band gap energy; Photoacoustic spectroscopy; Molecular beam epitaxy

1. Introduction

Recently, the investigations of doped $Al_xGa_{1-x}As$ alloys have been devoted to the optical and electrical properties, mainly due to their technical importance in fabrication of modern opto–electronic devices [1–5]. The efficiency of these devices is strongly affected by the incorporation of impurities and variation of alloy composition as well [1–4]. Experiments on doped semiconductors, above the Mott transition, reveal a band gap shift (BGS) beyond 10% of the band gap of the pure material [6–10].

2. Experimental methods

The doped $Al_xGa_{1-x}As$ samples, with different silicon concentrations (i.e. 1.0×10^{17} and 5.6×10^{17} cm^{-3}) were grown by molecular beam epitaxy (MBE) at 620°C on a semiinsulating [001]-

*Corresponding author. Permanent address: Instituto Nacional de Pesquisas Espaciais, INPE/LAS, C.P 515, 12201-970, São José dos Campos, SP, Brazil.

0167-9317/98/$19.00 © 1998 Published by Elsevier Science B.V. All rights reserved.
PII: S0167-9317(98)00201-9

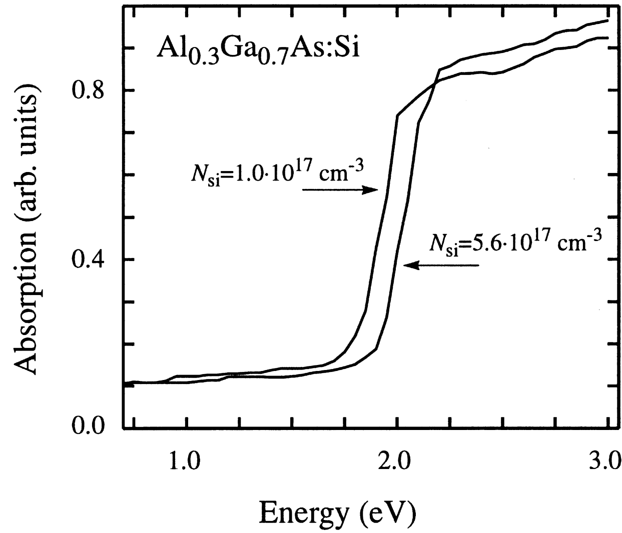

Fig. 1. PA intensity spectra of $Al_{0.3}Ga_{0.7}As$:Si for two silicon concentrations.

orientated Cr-doped GaAs substrate with the following layer sequence: a 0.3 μm thick undoped GaAs buffer, a 0.5 μm thick undoped AlGaAs buffer, the active 3.0 μm thick silicon-doped $Al_xGa_{1-x}As$ layer and a 60 Å thick silicon-doped GaAs cap layer. The latter one was removed in the experiment. The aluminum fraction of 30% ($x = 0.3$) for both samples, was measured by the reflection high energy electro–diffraction (RHEED) technique [5].

The measurement are done by the photoacoustic (PA) spectroscopy, which is a nondestructive spectroscopy technique for characterizing different kind of semiconductor materials. The spectra are obtained directly from the heat generated in a sample, due to nonradioactive absorption processes [3,11]. To obtain the optical band gap energy E_g^2, we have evaluated the derivative of the intensity signal near the fundamental absorption edge [12], leading to E_g^2. The room temperature (RT) PA intensity spectra for different $Al_{0.3}Ga_{0.7}As$:Si samples, as a function of photon energy, are shown in Fig. 1. The direct optical energy gaps for $N_{si} = 1.0 \times 10^{17}$ and 5.6×10^{17} cm^{-3} are obtained as $E_g^2 = 1.75$ and 1.86 eV, respectively. As a comparison, the band gap E_g^0 for undoped $Al_xGa_{1-x}As$ at 300 K and as a function of composition, extracted from Pavesi and Guzzi [4], is:

$$E_g^0(x) = 1.425 + 1.444x \text{ (eV)}. \tag{1}$$

For $x = 0.3$ it gives $E_g^0 = 1.858$ eV, closely to the experimental finding $E_g^0 = 1.843$ eV [13].

3. Discussion and results

Here we also investigated the BGS of the $Al_xGa_{1-x}As$ alloys theoretically as a function of both impurity concentration N and alloy composition x using RT crystal parameters. The applied calculation method is straightforward according to Jain and Roulston [9].

In order to identify the range of the BGS we have to know the impurity critical concentration N_c (Mott transition) as well as the solubility limit of the dopant in the material. The solubility limit of Si

as donor in $Al_xGa_{1-x}As$ is controversial. It has been neglected in the majority of earlier published investigations. For GaAs:Si it is around 7×10^{18} cm^{-3}, decreasing with the aluminum composition [5].

The value of N_c is calculated using a random-like donor distribution with the probability that the nearest donor neighbour lies at a certain distance R [10]. For $x=0$, corresponding to GaAs:Si, we have obtained $N_c=1.3\times10^{16}$ cm^{-3}. For $x=0.3$, corresponding to $Al_{0.3}Ga_{0.7}As$:Si, $N_c=4.2\times10^{16}$ cm^{-3}. Both values are calculated using the effective mass approximation, with the donor ionization energy at the Γ-point of the Brillouin zone [4].

Varying x from 0 to 1, the fundamental band gap of this material changes from GaAs to AlAs, i.e. from direct to indirect at a crossover composition at about $x=0.4$, where the X-point minima of the conduction band get lower in energy than the minimum at the Γ-point. An additional characteristic of this scenario is that, increasing the impurity concentration the population of the different minima at L, Γ and X-points lead also to variation of E_g. In Fig. 2 we show a schematic illustration of these conduction band minima.

We calculate the reduced band gap energy at the Γ-point as:

$$E_g^1 = E_g^0 - \Delta E_g, \tag{2}$$

where E_g^0 is the band gap for undoped material, as given by Eq. (1) and ΔE_g is the BGS. As a first attempt we define the optical band gap at the Γ-point as:

$$E_g^2 = E_g^1 + \Delta E_g^{BM}, \tag{3}$$

where ΔE_g^{BM} is the Burstein–Moss shift [14,15], which is given by:

$$\Delta E_g^{BM} = \Delta E_F(1 + m_{dM}/m_{dm}), \tag{4}$$

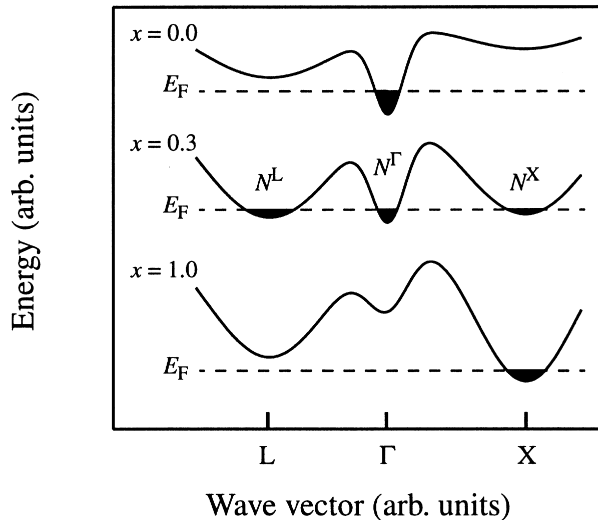

Fig. 2. Schematic illustration of the populated conduction band minima at different x. N^{Γ}, N^{L} and N^{X} are the electron concentrations in a Γ-, L- and X-valley, respectively.

Here, m_{dM} and m_{dm} are the density of states effective masses of majority and minority carriers, respectively, and ΔE_F is the shift in Fermi energy due to population of free carriers in the conduction band. ΔE_g as a function of composition and of the electron concentration in the conduction band minimum at the Γ-point, N^Γ, is obtained from [9]:

$$\Delta E_g(N,x) = A_1(x)N^{\Gamma^{1/3}} + A_2(x)N^{\Gamma^{1/4}} + A_3(x)N^{\Gamma^{1/2}} \text{ (eV)}, \tag{5}$$

where

$$A_1(x) = 40.14 a_0 \varepsilon_0(x)^{-1} \tag{6a}$$

$$A_2(x) = 18.49 a_0^{3/4} \varepsilon_0(x)^{-5/4} m_{dM}(x)^{1/4} \tag{6b}$$

$$A_3(x) = 43.72 a_0^{3/2} \varepsilon_0(x)^{-1/2} m_{dM}(x)^{-1/2}[1 + m_{dm}(x)/m_{dM}(x)]. \tag{6c}$$

In the equations above, a_0 is the Bohr radius and $\varepsilon_0(x)$ is the static dielectric constant. For small impurity concentrations $N^\Gamma = N$, but when the impurity concentration is increased the L- and the X-valleys will start to be populated and N^Γ will then be smaller than N. The coefficients A_1, A_2 and A_3 represent the exchange energy, correlation energy and electron-impurity scattering, respectively [6,9,16]. In Eqs. (4), (6a)–(6c) we have used:

$$\varepsilon_0(x) = 12.85 - 2.79x \tag{7a}$$

$$m_{dM}(x) = 0.063 + 0.083x \tag{7b}$$

$$m_{dm}(x) = 0.288 + 0.139x \tag{7c}$$

which are presumed to be valid at RT [4,17].

In Fig. 3 we show, in three dimensions (3D), the variation of ΔE_g^{BM} as a function of N and x. The solid line marked $N_s^L(x)$ indicates at which concentrations the L-valleys start to be populated. In Fig. 4 we show E_g^1 and E_g^2 as a function of N for $x=0$, 0.30 and 0.36. The full circles correspond to PA measurements. The theoretical calculation presents a rough agreement with these data in this range of concentration. Both E_g^1 and E_g^2 have similar behaviour as observed in n-type Si and Ge [7–10]. The energy gap E_g^1 decreases with N presenting two bendings $N_s^L(x)$ and $N_s^X(x)$ at certain values for a specific x.

These bendings are due to the onset of populating of the L- and X-valleys [16]. For instance, for $x=0$, 0.3 and 0.36 the L-valleys start to be populated at $N=1.0\times10^{19}$, 2.3×10^{18} and 7.8×10^{17} cm^{-3}, corresponding to $E_g^1=1.05$, 1.71 and 1.85 eV, and the X-valleys start to be populated at $N=2.1\times10^{20}$, 2.4×10^{19} and 3.3×10^{18} cm^{-3}, corresponding to $E_g^1=0.85$, 1.65 and 1.84 eV. For the data shown in Fig. 4 there is evidently a striking dependence of the band gap modifications on the composition x. Thus, the effects of doping are much less pronounced at $x\approx0.3$ than at $x=0$. The reason for this is simple. The Burstein–Moss shift is smaller at $x\approx0.3$ because the electrons are distributed over many valleys giving a smaller E_F. As many valleys become occupied the screening from the electron gas gets larger and more effectively screens electron–electron and electron–ion interactions.

In Fig. 5 we show, in 3D, E_g^1 as a function of N and x. The solid line marked $N_s^L(x)$ indicates at

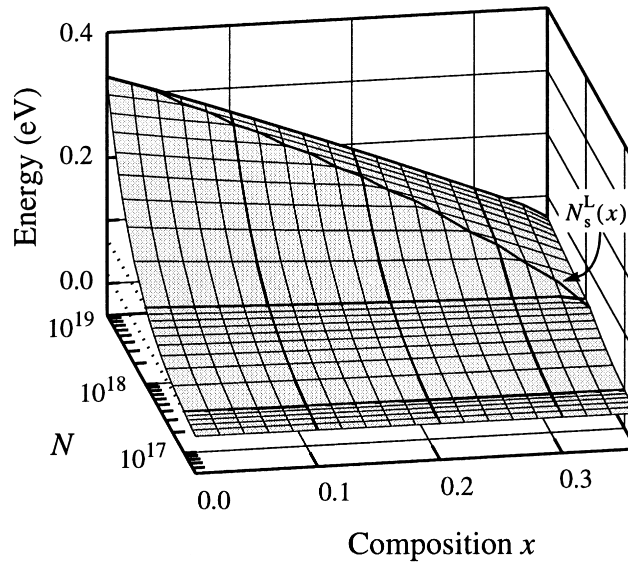

Fig. 3. Calculated Burstein–Moss shift, defined in Eq. (4), as a function of aluminum composition and impurity concentration. The solid line marked $N_s^L(x)$ indicates at which concentrations the L-valleys start to be populated.

which concentrations the L-valleys start to be populated. It can be seen that the effect of the L-valleys is of importance for high impurity concentrations or for high composition value x. If the composition is above $x=0.4$ the global minimum is located at the X point of the Brillouin zone. The three

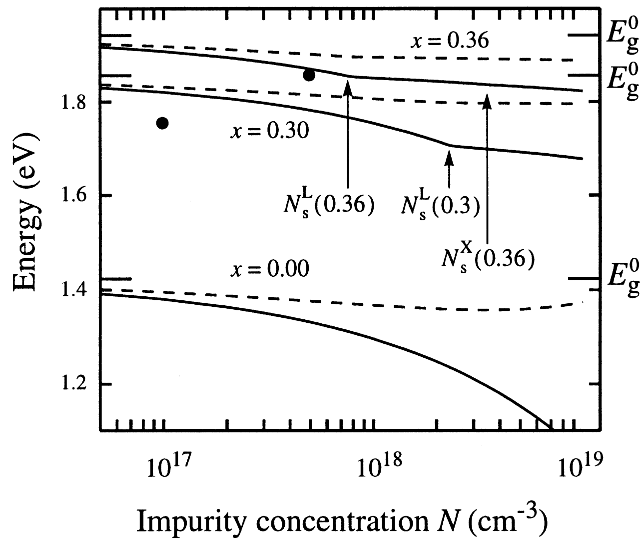

Fig. 4. Calculated reduced band gap energies E_g^1 (solid lines) and optical band gap energies E_g^2 (dashed lines) for $x=0$, 0.3 and 0.36. The band gaps for undoped $Al_xGa_{1-x}As$ are $E_g^0=1.425$, 1.858 and 1.945 eV for the three compositions, respectively. $N_s^L(x)$ is the concentration at which the L-valleys start to be populated. $N_s^X(x)$ is the concentration at which the X-valleys start to be populated. Full circles are the experimental data for the composition $x=0.3$.

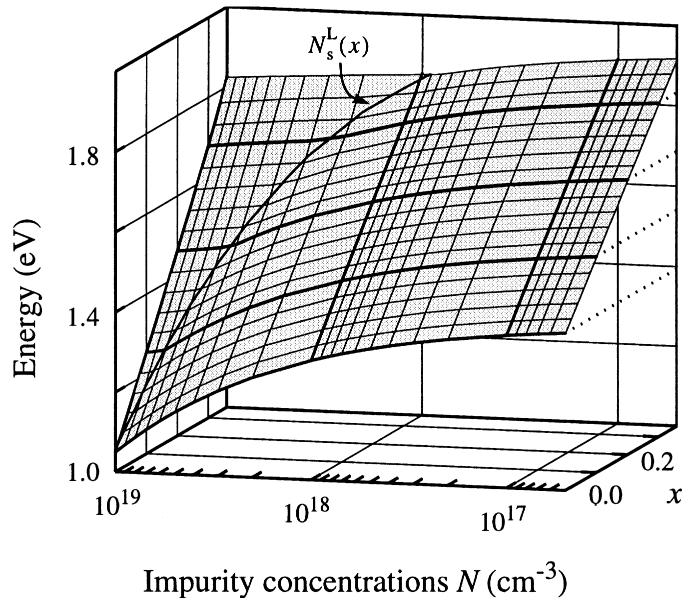

Fig. 5. Calculated reduced band gap energies for compositions $0 \leq x \leq 0.36$ and impurity concentrations $5.0 \times 10^{16} \leq N \leq 1.0 \times 10^{19}$ cm^{-3}. The solid line marked $N_s^L(x)$ indicates at which concentrations the L-valleys start to be populated (see also Fig. 4).

equivalent X-valleys strongly dominate in this region and the Γ- and L-valleys have only a minor effect on the BGS [16]. Furthermore, for a given impurity concentration the BGS for $x = 1.0$ is smaller than for $x = 0.0$, due to the higher density of states effective mass in the three X-valleys than in the single Γ-valley.

Acknowledgements

This work was financially supported by the Brazilian National Research Council (CNPq), the Swedish Board for Industrial and Technical Development (NUTEK) and the Swedish Research Council for Engineering Sciences (TFR). Discussions with J. Caetano de Souza in an earlier stage of the PA experiments are also acknowledged.

References

[1] N. Galbiati, E. Grilli, M. Guzzi, L. Brusaferri, L. Pavesi, M. Henini, Semicond. Sci. Technol. 11 (1996) 1830–1837.
[2] N. Galbiati, L. Pavesi, E. Grilli, M. Guzzi, M. Henini, Appl. Phys. Lett. 69 (1996) 4215–4217.
[3] A. Ferreira da Silva, A.G. de Oliveira, J. Caetano de Souza, A.V. Batista da Silva, P. César Farias, A. Santos Alves, I. Pepe, Phantoms Newslett. 11 (1996) 2–3.
[4] L. Pavesi, M. Guzzi, J. Appl. Phys. 75 (1994) 4779–4842.
[5] A.G. de Oliveira, G.A.M. Sáfar, J.F. Sampaio, Braz. J. Phys. 24 (1994) 363–369.
[6] K.-F. Berggren, B.E. Sernelius, Phys. Rev. B 24 (1981) 1971–1986.

[7] K.-F. Berggren, B.E. Sernelius, Solid State Electron. 28 (1985) 11–15.
[8] J. Wagner, J.A. del Alamo, J. Appl. Phys. 63 (1988) 425–429.
[9] S.C. Jain, D.J. Roulston, Solid State Electron. 34 (1991) 453–465.
[10] P. Nubile, A. Ferreira da Silva, Solid State Electron. 41 (1997) 121–124.
[11] A. Ferreira da Silva, N. Veissid, C.Y. An, I. Pepe, N.B. de Oliveira, A.V. Batista da Silva, Appl. Phys. Lett. 69 (1996) 1930–1932.
[12] I. Hamberg, C.G. Granqvist, K.-F. Berggren, B.E. Sernelius, L. Engström, Phys. Rev. B 30 (1984) 3240–3249.
[13] M. El Allali, C.B. Sørensen, E. Veje, P. Tidemand-Petersson, Phys. Rev. B 48 (1993) 4398–4404.
[14] E. Burstein, Phys. Rev. 93 (1954) 632–633.
[15] T.M. Moss, Proc. Phys. Soc. London Ser. B 67 (1954) 775–782.
[16] C. Persson, A. Ferreira da Silva, K.-F. Berggren, (to appear).
[17] Landolt–Börnstein, Numerical Data and Functional Relationship; in: D. Madelung, M. Schulz (Eds.), Science and Technology, New Series, III/22a, Springer, Berlin, 1987.